ARTICLES
PUBLISHED ONLINE: 11 JULY 2010 | DOI: 10.1038/NCHEM.731
nature chemistry

Crystal structure of a metal ion-bound oxoiron(IV) complex and implications for biological electron transfer

Shunichi Fukuzumi[1,2]*, Yuma Morimoto[1], Hiroaki Kotani[1], Panče Naumov[1], Yong-Min Lee[2,3] and Wonwoo Nam[2,3]*

Critical biological electron-transfer processes involving high-valent oxometal chemistry occur widely, for example in haem proteins [oxoiron(IV); $Fe^{IV}(O)$] and in photosystem II. Photosystem II involves Ca^{2+} as well as high-valent oxomanganese cluster species. However, there is no example of an interaction between metal ions and oxoiron(IV) complexes. Here, we report new findings concerning the binding of the redox-inactive metal ions Ca^{2+} and Sc^{3+} to a non-haem oxoiron(IV) complex, $[(TMC)Fe^{IV}(O)]^{2+}$ (TMC = 1,4,8,11-tetramethyl-1,4,8,11-tetraazacyclotetradecane). As determined by X-ray diffraction analysis, an oxo-Sc^{3+} interaction leads to a structural distortion of the oxoiron(IV) moiety. More importantly, this interaction facilitates a two-electron reduction by ferrocene, whereas only a one-electron reduction process occurs without the metal ions. This control of redox behaviour provides valuable mechanistic insights into oxometal redox chemistry, and suggests a possible key role that an auxiliary Lewis acid metal ion could play in nature, as in photosystem II.

Metal ions play pivotal roles in biological electron-transfer (ET) systems such as photosynthesis and respiration[1–6]. Oxoiron(IV) interactions occur widely in enzymes, facilitating oxidative processes using molecular oxygen or hydrogen peroxide[1–3]. Another very important example is the oxygen-evolving complex (OEC) of photosystem II (PS II), in which Ca^{2+} acts as an essential cofactor in the manganese–calcium (Mn_4Ca) active site responsible for Earth's molecular oxygen, via oxygen evolution in photosynthesis[4–11]. Although high-valent oxomanganese(V) species are considered to be reactive intermediates in O–O bond formation by means of the OEC of PS II, the exact functional role of Ca^{2+} remains unclear[4–11]. In biomimetic studies, a number of high-valent oxometal intermediates have been synthesized as chemical models of the reactive intermediates that are involved in biological redox reactions[12–16]. However, the possible control of oxo-transfer or redox chemistry of high-valent oxometal intermediates by the binding of redox-inactive metal ions appears not to be known or even to have been considered. On the other hand, redox-inactive metal ions such as Ca^{2+} have been established to control the redox reactivity of organic electron acceptors by binding to the one-electron reduced species involved, that is, radical anions of electron acceptors[17–19].

Here, we report the first example of binding of metal ions such as Sc^{3+} and Ca^{2+} to a non-haem oxoiron(IV) complex, $[(TMC)Fe^{IV}(O)]^{2+}$ (TMC = 1,4,8,11-tetramethyl-1,4,8,11-tetra-azacyclotetradecane)[20]; the crystal structure of Sc^{3+}-bound $[(TMC)Fe^{IV}(O)]^{2+}$ was determined by X-ray crystallography. The binding of Sc^{3+} to $[(TMC)Fe^{IV}(O)]^{2+}$ results in a change in the number of electrons transferred from ferrocene (Fc) to the oxoiron complex: two-electron reduction of $[(TMC)Fe^{IV}(O)]^{2+}$ by Fc occurs with Sc^{3+} binding, but only single-electron reduction of $[(TMC)Fe^{IV}(O)]^{2+}$ by Fc occurs in the absence of Sc^{3+} (ref. 21). Such a change in the number of electrons by binding of a metal ion to high-valent oxometal species provides valuable insight into the role of metal ions at the active site of the OEC.

Results and discussion

We have shown recently that ET from one-electron reductants, such as Fc and its derivatives, to $[(TMC)Fe^{IV}(O)]^{2+}$ occurs in acetonitrile

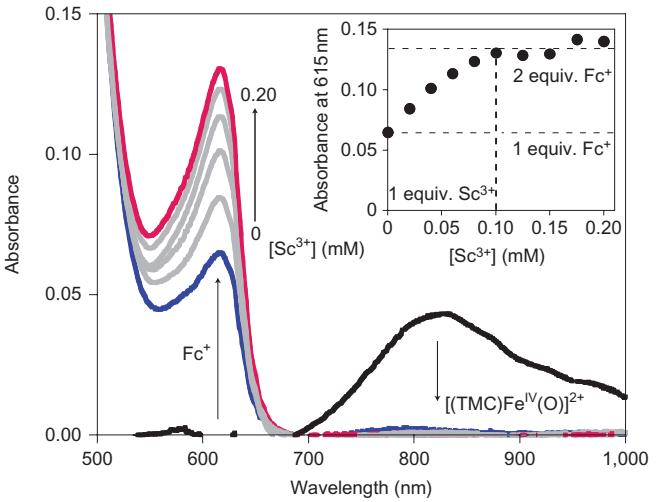

Figure 1 | Sc^{3+} effect on the ET reaction of $[(TMC)Fe^{IV}(O)]^{2+}$. Spectral changes observed in ET from Fc (5.0 mM) to $[(TMC)Fe^{IV}(O)]^{2+}$ (0.10 mM) in the presence of various concentrations of Sc^{3+} (0 mM, blue line; 0.02–0.08 mM, grey lines; 0.2 mM, red line) in MeCN. Inset: titration curve showing a stoichiometry of $[Fc^{+}]$ with respect to $[Sc^{3+}]$.

[1]Department of Material and Life Science, Division of Advanced Science and Biotechnology, Graduate School of Engineering, Osaka University, SORST, Japan Science and Technology Agency (JST), Suita, Osaka 565-0871, Japan, [2]Department of Bioinspired Science, Ewha Womans University, Seoul 120-750, Korea, [3]Department of Chemistry and Nano Science, Center for Biomimetic Systems, Ewha Womans University, Seoul 120-750, Korea.
*e-mail: fukuzumi@chem.eng.osaka-u.ac.jp; wwnam@ewha.ac.kr

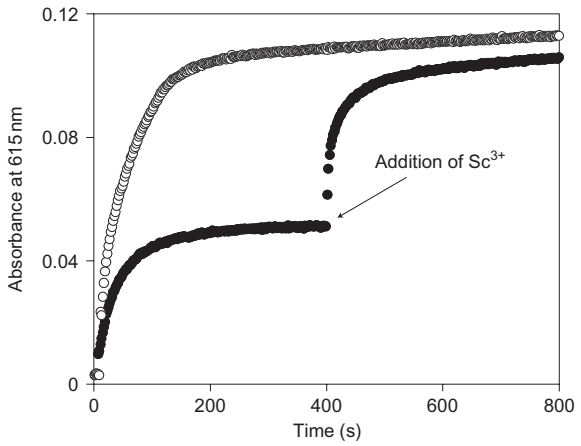

Figure 2 | Kinetic measurements of ET from Fc to $[(TMC)Fe^{IV}(O)]^{2+}$. Time profiles of the absorption change at $\lambda = 615$ nm due to Fc^{+} observed in ET from Fc (5.0 mM) to $[(TMC)Fe^{IV}(O)]^{2+}$ (0.10 mM) in a de-aerated MeCN at 298 K. Sc^{3+} (0.20 mM) (closed circles) was added after completion of the one-electron reduction of $[(TMC)Fe^{IV}(O)]^{2+}$, as indicated by the arrow. Sc^{3+} (0.10 mM) (open circles) was added from the start of the reaction.

(MeCN), thereby producing the ferrocenium cation (Fc^{+}) and $[(TMC)Fe^{III}(O)]^{+}$ (ref. 21). Interestingly, when we carried out the ET reaction in the presence of scandium triflate [$Sc(OTf)_3$] ($OTf = OSO_2CF_3$), we observed two-electron reduction of $[(TMC)Fe^{IV}(O)]^{2+}$ by Fc to give two equivalents of Fc^{+} (see solid red line in Fig. 1). The temporal profile of ET from Fc to $[(TMC)Fe^{IV}(O)]^{2+}$ is shown in Fig. 2, where one equivalent of Fc^{+} is formed. By addition of Sc^{3+} to the resulting solution, the additional ET occurs to produce one more equivalent of Fc^{+} (see the arrow in Fig. 2). When Sc^{3+} is present from the beginning, two equivalents of Fc^{+} are formed as a one-step process in the two-electron reduction of $[(TMC)Fe^{IV}(O)]^{2+}$ by Fc (Fig. 2). The two-electron reduction of $[(TMC)Fe^{IV}(O)]^{2+}$ by Fc was also observed in the presence of $Ca(OTf)_2$. In this case, however, a large excess of Ca^{2+} (4.0 mM) was required to complete the two-electron reduction of $[(TMC)Fe^{IV}(O)]^{2+}$ (0.10 mM), probably due to the lower Lewis acidity of Ca^{2+} compared to the Sc^{3+} ion[22,23].

The rate of formation of Fc^{+} in the presence of Sc^{3+} obeys pseudo-first-order kinetics, and the pseudo-first-order rate constant (k_{obs}) increases linearly with increasing concentration of Fc (see Supplementary Fig. S1). The ET rate constant (k_{et}) was determined from the slope of the linear plot. The pseudo-first-order kinetics for the two-electron reduction of $[(TMC)Fe^{IV}(O)]^{2+}$ by Fc in the presence of Sc^{3+} indicates that the first ET from Fc to $[(TMC)Fe^{IV}(O)]^{2+}$ is the rate-determining step, followed by the rapid second ET from Fc to the $[(TMC)Fe^{III}(O)]^{+}/Sc^{3+}$ complex to produce one additional equivalent of Fc^{+} and $[(TMC)Fe^{II}(O)]/Sc^{3+}$. We also found that the k_{et} value in the presence of Sc^{3+} is smaller than the value in the absence of Sc^{3+}, remaining constant at Sc^{3+} concentrations higher than one equivalent (Fig. 3a). This may result from the larger reorganization energy of ET associated with binding of Sc^{3+} to $[(TMC)Fe^{IV}(O)]^{2+}$. This conclusion is confirmed by measurements of the temperature dependence of k_{et} in the absence and presence of Sc^{3+}, which correspond to activation enthalpies of 57 and 71 kJ mol^{-1}, respectively (Fig. 3b).

A question to be answered here is why the two-electron reduction of $[(TMC)Fe^{IV}(O)]^{2+}$ with Fc is made possible by the presence of redox-inactive metal ions. If the $Fe^{IV}(O)$ complex is reduced to the $Fe^{III}(O)$ complex, the binding of Sc^{3+} to the oxo group is expected to become stronger due to increased electron density on the oxo group. This would facilitate further reduction to an Fe^{II} complex, accompanied by removal of the oxo group with protons as water (Fig. 1).

We have shown the 1:1 stoichiometry of Sc^{3+} to $[(TMC)Fe^{IV}(O)]^{2+}$ in the two-electron reduction of $[(TMC)Fe^{IV}(O)]^{2+}$ by Fc in the presence of Sc^{3+} (Figs 1 and 3a) and there is no change in the k_{et} value with increasing Sc^{3+} concentration. Definitive proof for Sc^{3+} binding to the oxo group of $[(TMC)Fe^{IV}(O)]^{2+}$ was obtained from X-ray crystallography. Single crystals of $[(TMC)Fe^{IV}(O)–Sc(OTf)_4(OH)]$ were grown from a MeCN/diethyl ether mixture at −15 °C. The X-ray crystal structure in Fig. 4 clearly shows the binding of Sc^{3+} to the oxo moiety of $[(TMC)Fe^{IV}(O)]^{2+}$ (see Supplementary Information for crystallographic data and refinement details (Supplementary Tables S1–S4) and also Supplementary Fig. S2 for the asymmetric unit of the complex). To the best of our knowledge, this is the first high-valent oxometal species binding a metal ion at the oxometal moiety. The strong binding of Sc^{3+} to the oxo group results in elongation of the Fe–O distance of the $Fe^{IV}(O)–Sc^{3+}$ complex

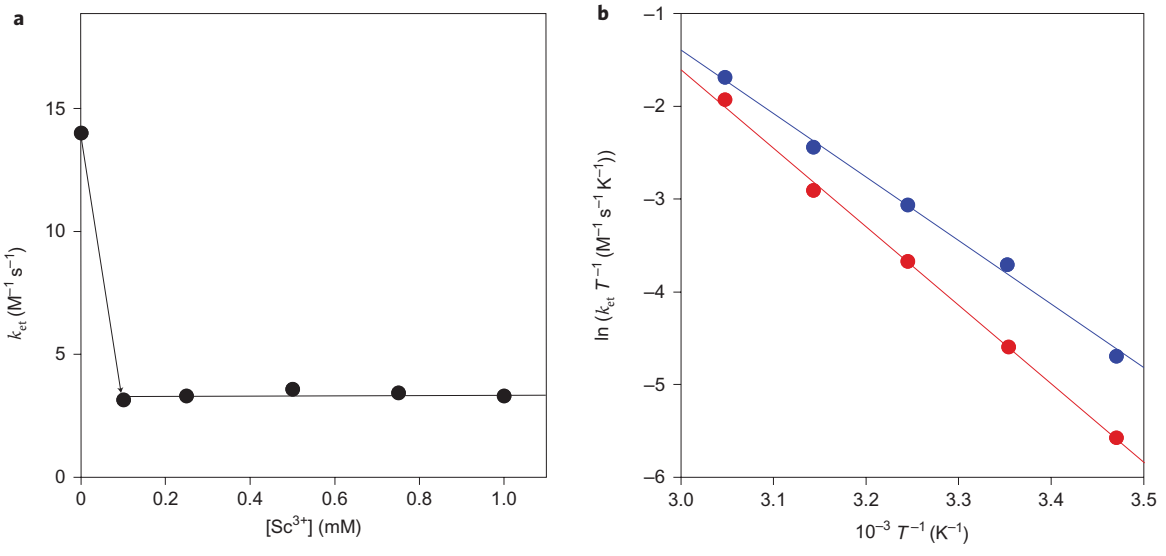

Figure 3 | Temperature dependence on the ET rate constants. a, Plot of the pseudo-first-order rate constant (k_{et}) versus concentration of Sc^{3+} in ET from Fc (5.0 mM) to $[(TMC)Fe^{IV}(O)]^{2+}$ (0.10 mM) in the presence of Sc^{3+} in MeCN at 298 K. **b**, Eyring plots of the rate constant of ET from Fc (5.0 mM) to $[(TMC)Fe^{IV}(O)]^{2+}$ (0.10 mM) in the absence (blue circles) and presence of Sc^{3+} (red circles) in MeCN at various temperatures.

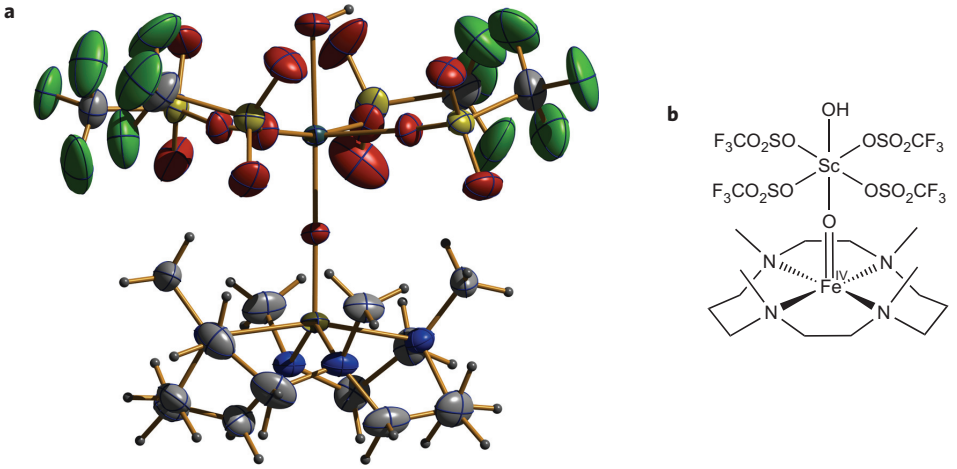

Figure 4 | Sc^{3+}-bound (TMC)Fe^{IV}(O) complex. a,b, Oak Ridge Thermal Ellipsoid Plot (ORTEP)-style (**a**) and chemical structure (**b**) plots of the Sc^{3+}-bound non-haem oxoiron(IV) complex, [(TMC)Fe^{IV}(O)-Sc(OTf)$_4$(OH)]: $a = 12.3656(11)$ Å, $b = 16.4492(13)$ Å, $c = 19.9866(17)$ Å, $\beta = 94.337(4)^\circ$, $V = 4053.7(6)$ Å^3, monoclinic, $P2_1/n$, $Z = 4$, $R_1 = 0.0590$, $wR_2 = 0.1862$, $S = 1.030$. The displacement ellipsoids are drawn at the 30% probability level.

(1.754(3) Å), and the Fe–O distances of [(TMC)Fe^{IV}(O)(NCMe)]$^{2+}$, [(TMCS)Fe^{IV}(O)]$^{+}$ (TMCS = 1-mercaptoethyl-4,8,11-trimethyl-1,4,8,11-tetraazacyclotetradecane) and [(TMC-py)Fe^{IV}(O)]$^{2+}$ (TMC-py = 1-(2′-pyridylmethyl)-4,8,11-trimethyl-1,4,8,11-tetraazacyclotetradecane) were reported to be 1.643(3) Å by X-ray crystallography, 1.70(2) Å by density functional theory (DFT) calculations and 1.667(3) Å by X-ray crystallography, respectively[20,24,25]. Here, the Sc^{3+}–O (oxo) bond length within the Fe^{IV}(O)–Sc^{3+} moiety is 1.933(3) Å, which is significantly shorter than the Sc^{3+}–OH (hydroxo) distance (2.188(3) Å), a clear indication of stronger binding of Sc^{3+} to the oxo group when compared to the hydroxo group. The Fe–N bonds in the Fe^{IV}(O)–Sc^{3+} complex range from 2.132(3) to 2.210(4) Å and average 2.175 Å, which is longer than the average value (2.095 Å) of the Fe^{IV}(O) complex without Sc^{3+}.

By removal of the coordinated MeCN from octahedral six-coordinate [(TMC)Fe^{IV}(O)(NCMe)]$^{2+}$ (Fig. 5a)[20] via Sc^{3+} coordination, the iron atom in the Fe^{IV}(O)–Sc^{3+} complex adopts a distorted square pyramidal five-coordinated geometry (Fig. 5b). All four *N*-methyl groups of the TMC ligand in the Fe^{IV}(O)–Sc^{3+} complex point to the same side of the oxo moiety (Fig. 4b), whereas those in the Fe^{IV}(O) complex without Sc^{3+} point away from the oxo ligand, below the plane defined by the four nitrogens of the TMC ligand and *anti* to the oxo atom[20]. Such switching of the four *N*-methyl groups in the binding site of the oxo group from *anti* to *syn* has been recently suggested to occur by treatment of [(TMC)Fe^{IV}(O)(NCMe)]$^{2+}$ with PhIO in the presence of tetrafluoroborate anion, although the X-ray crystal structure has yet to be determined[26]. In the *syn* structure there is enough space to accommodate the Sc^{3+} complex bound to the oxo moiety, whereas there is

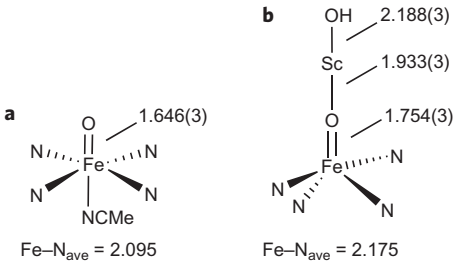

Figure 5 | Comparison of the (TMC)Fe^{IV}(O) complex and the Sc^{3+}-bound (TMC)Fe^{IV}(O) complex. a,b, Structures and selected bond lengths (in ångströms) of (TMC)Fe^{IV}(O)(NCMe) (**a**) and [(TMC)Fe^{IV}(O)-Sc(OTf)$_4$(OH)](MeCN) (**b**). The TMC and OTf^- ligands have been omitted for clarity.

no space for the axial binding of MeCN in the *trans* position to the iron-oxo moiety. The mechanism of the structural change from *anti* to *syn* accompanied by binding of Sc^{3+} and removal of the coordinated MeCN has yet to be clarified.

In conclusion, we have isolated and determined the crystal structure of the Fe^{IV}(O)–Sc^{3+} complex. The strong binding of Sc^{3+} to the oxo group results in significant structural change from an octahedrally hexacoordinated metal centre to a pentacoordinated one with square pyramidal coordination, with concomitant switching of the four *N*-methyl groups of the TMC ligand at the binding site of the oxo group from *anti* to *syn* disposition. A dramatic effect on redox properties occurs, in which the number of electrons transferred from Fc to the Fe^{IV}(O) complex is also changed from one to two, depending on the binding of Sc^{3+} or Ca^{2+} to the oxo group. These findings suggest a likely role for a redox-inactive metal ion as a necessary or useful component in chemical or natural systems, for the modulation of redox potential and ET properties of high-valent oxometal species. This could be considered in discussions of the unknown role of the Ca^{2+} ion found in the vicinity of the active site of OEC, that is, its facilitation of the two-electron reduction of a Mn^{V}=O group by water/hydroxide.

Methods

See experimental section in Supplementary Information for detailed experimental conditions and procedures, spectroscopic and kinetics analyses, and crystal data.

Received 30 December 2009; accepted 24 May 2010; published online 11 July 2010

References

1. Kaim, W. & Schwederski, B. *Bioinorganic Chemistry: Inorganic Elements in the Chemistry of Life* (Wiley, 1994).
2. Kovacs, J. A. How iron activates O_2. *Science* **299,** 1024–1025 (2009).
3. Ferguson-Miller, S. & Babcock, G. T. Heme/copper terminal oxidases. *Chem. Rev.* **96,** 2889–2908 (1996).
4. Diner, B. A. & Babcock, G. T. *Oxygenic Photosynthesis: The Light Reactions* (Kluwer Academic Publishers, 1996).
5. Yagi, M. & Kaneko, M. Molecular catalysts for water oxidation. *Chem. Rev.* **101,** 21–36 (2001).
6. McEvoy, J. P. & Brudvig, G. W. Water-splitting chemistry of photosystem II. *Chem. Rev.* **106,** 4455–4483 (2006).
7. Ferreira, K. N. *et al.* Architecture of the photosynthetic oxygen-evolving center. *Science* **303,** 1831–1838 (2004).
8. Loll, B. *et al.* Towards complete cofactor arrangement in the 3.0 Å resolution structure of photosystem II. *Nature* **438,** 1040–1044 (2005).
9. Yano, J. *et al.* Where water is oxidized to dioxygen: structure of the photosynthetic Mn_4Ca cluster. *Science* **314,** 821–825 (2006).

10. Sporoviero, E. M. *et al.* Quantum mechanics/molecular mechanics study of the catalytic cycle of water splitting in photosystem II. *J. Am. Chem. Soc.* **130,** 3428–3442 (2008).
11. Barber, J. Photosynthetic energy conversion: natural and artificial. *Chem. Soc. Rev.* **38,** 185–196 (2009).
12. Que, L. Jr The road to non-heme oxoferryls and beyond. *Acc. Chem. Res.* **40,** 493–500 (2007).
13. Nam, W. High-valent iron(IV)–oxo complexes of heme and non-heme ligands in oxygenation reactions. *Acc. Chem. Res.* **40,** 522–531 (2007).
14. Sono, M., Roach, M. P., Coulter, E. D. & Dawson, J. H. Heme-containing oxygenases. *Chem. Rev.* **96,** 2841–2887 (1996).
15. Meunier, B. (ed.) *Metal-Oxo and Metal-Peroxo Species in Catalytic Oxidations* (Springer-Verlag, 2000).
16. Ortiz de Montellano, P. R. (ed.) *Cytochrome P450: Structure, Mechanism, and Biochemistry* (Kluwer Acaemic/Plenum Publishers, 2005).
17. Fukuzumi, S. Roles of metal ions in controlling bioinspired electron-transfer systems. Metal ion-coupled electron transfer. *Prog. Inorg. Chem.* **56,** 49–153 (2009).
18. Fukuzumi, S. Catalysis on electron transfer and the mechanistic insight into redox reactions. *Bull. Chem. Soc. Jpn* **70,** 1–28 (1997).
19. Fukuzumi, S. New perspective of electron transfer chemistry. *Org. Biomol. Chem.* **1,** 609–620 (2003).
20. Rohde, J.-U. *et al.* Crystallographic and spectroscopic characterization of a nonheme Fe(IV)=O complex. *Science* **299,** 1037–1039 (2003).
21. Lee, Y.-M. *et al.* Fundamental electron-transfer properties of non-heme oxoiron(IV) complexes. *J. Am. Chem. Soc.* **130,** 434–435 (2008).
22. Fukuzumi, S. & Ohkubo, K. Quantitative evaluation of Lewis acidity of metal ions derived from the g-values of ESR spectra of superoxide–metal ion complexes in relation with the promoting effects in electron transfer reactions. *Chem. Eur. J.* **6,** 4532–4535 (2000).
23. Fukuzumi, S. & Ohkubo, K. Fluorescence maxima of 10-methylacridone–metal ion salt complexes: a convenient and quantitative measure of Lewis acidity of metal ion salts. *J. Am. Chem. Soc.* **124,** 10270–10271 (2002).
24. Bukowski, M. R. *et al.* A thiolate-ligated nonheme oxoiron(IV) complex relevant to cytochrome P450. *Science* **310,** 1000–1002 (2005).
25. Thibon, A. *et al.* Proton- and reductant-assisted dioxygen activation by a nonheme iron(II) complex to form an oxoiron(IV) intermediate. *Angew. Chem. Int. Ed.* **47,** 7064–7067 (2008).
26. Ray, K. *et al.* An inverted and more oxidizing isomer of $[Fe^{IV}(O)(tmc)(NCCH_3)]^{2+}$. *Angew. Chem. Int. Ed.* **47,** 8068–8071 (2008).

Acknowledgements

This work was supported by a Grant-in-Aid (no. 20108010 to S.F.) and a Global COE program, 'the Global Education and Research Center for Bio-Environmental Chemistry' from the Ministry of Education, Culture, Sports, Science and Technology, Japan (to S.F.), and NRF/MEST through a WCU project (R31-2008-000-10010-0) (to S.F. and W.N.) and the Creative Research Initiatives Program (to W.N.). Crystallographic data for $[(TMC)Fe^{IV}(O)–Sc(OTf)_4(OH)]$ have been deposited with the Cambridge Crystallographic Data Center under reference numbers CCDC-742067 (X-ray).

Author contributions

S.F., Y.M., H.K. and W.N. conceived and designed the experiments. Y.M. and P.N. performed the experiments. Y.M., H.K. and P.N. analysed the data. P.N. and Y.M.L. contributed materials and analysis tools. S.F. and W.N. co-wrote the paper.

Additional information

The authors declare no competing financial interests. Supplementary information accompanies this paper at www.nature.com/naturechemistry. Reprints and permission information is available online at http://npg.nature.com/reprintsandpermissions/. Correspondence and requests for materials should be addressed to S.F. and W.N.